



# HHS Public Access

Author manuscript

*Nanomedicine*. Author manuscript; available in PMC 2016 August 01.

Published in final edited form as:

*Nanomedicine*. 2015 August ; 11(6): 1377–1385. doi:10.1016/j.nano.2015.03.007.

## Aerosol Droplet Delivery of Mesoporous Silica Nanoparticles: A Strategy for Respiratory-Based Therapeutics

Xueting Li<sup>1,2,3</sup>, Min Xue<sup>4</sup>, Otto G. Raabe<sup>1,5</sup>, Holly L. Aaron<sup>6</sup>, Ellen A. Eisen<sup>7</sup>, James E. Evans<sup>1</sup>, Fred A. Hayes<sup>3</sup>, Sumire Inaga<sup>8</sup>, Abderrahmane Tagmout<sup>2</sup>, Minoru Takeuchi<sup>9</sup>, Chris Vulpe<sup>2</sup>, Jeffrey I. Zink<sup>4</sup>, Subhash H. Risbud<sup>3</sup>, and Kent E. Pinkerton<sup>1,\*</sup>

<sup>1</sup>Center for Health and the Environment, University of California, Davis, USA

<sup>2</sup>Department of Nutritional Sciences and Toxicology, University of California, Berkeley, USA

<sup>3</sup>Department of Chemical Engineering and Materials Science, University of California, Davis, USA

<sup>4</sup>Department of Chemistry and Biochemistry, University of California, Los Angeles, USA

<sup>5</sup>Department of Molecular Biosciences, University of California, Davis, USA

<sup>6</sup>Cancer Research Laboratory Molecular Imaging Center, University of California, Berkeley, USA

<sup>7</sup>Environmental Health Sciences, School of Public Health, University of California, Berkeley, USA

<sup>8</sup>Department of Functional, Morphological and Regulatory Science, Tottori University, Yonago, Japan

<sup>9</sup>Department of Animal Medical Science, Kyoto Sangyo University, Kyoto, Japan

### Abstract

A highly versatile nanoplatform that couples mesoporous silica nanoparticles (MSN) with an aerosol technology to achieve direct nanoscale delivery to the respiratory tract is described. This novel method can deposit MSN nanoparticles throughout the entire respiratory tract, including nasal, tracheobronchial and pulmonary regions using a water-based aerosol. This delivery method was successfully tested in mice by inhalation. The MSN nanoparticles used have the potential for carrying and delivering therapeutic agents to highly specific target sites of the respiratory tract. The approach provides a critical foundation for developing therapeutic treatment protocols for a wide range of diseases where aerosol delivery to the respiratory system would be desirable.

---

\***Corresponding Author.** Kent E. Pinkerton, Ph.D., Center for Health and the Environment, 1 Shields Avenue, Davis, CA 95616, USA, Phone: 530 752 8334, kepinkerton@ucdavis.edu.

**Publisher's Disclaimer:** This is a PDF file of an unedited manuscript that has been accepted for publication. As a service to our customers we are providing this early version of the manuscript. The manuscript will undergo copyediting, typesetting, and review of the resulting proof before it is published in its final citable form. Please note that during the production process errors may be discovered which could affect the content, and all legal disclaimers that apply to the journal pertain.

There are no competing interests.

X. Li presented preliminary findings of this research at the First International Translational Nanomedicine Conference in Boston, MA (2013).

## Keywords

mesoporous silica nanoparticles; aerosol droplets; respiratory tract

---

## Introduction

Multifunctional engineered silica nanocarriers can effectively transport a wide range of specific therapeutic agents to control delivery, timing, and precision of compounds to biological target sites<sup>1-7</sup>. However, their use via inhalation is currently limited by a general lack of technological development to deliver aerosolized nanoparticles that are inhalable and controllable for optimal delivery to selective sites throughout the respiratory tract. The need for efficiently designed nanocarrier systems is crucial to appropriately target a therapeutic compound and protect it so it could be released upon reaching the desired site<sup>8-11</sup>. This is especially true in the lung due to a complex airway geometry, variations in breathing patterns, specific cells at target sites and factors that affect particle deposition, including size, shape, charge and density.

Mesoporous silica nanoparticles (MSN) are inorganic-based nanocarriers developed for hydrophobic and hydrophilic drug molecules, as well as other therapeutic elements for controlled on-demand delivery in biological systems. MSN drug-carrier technology has advanced to the pre-clinical phase and shows significant potential for treating diseases by limiting side effects and controlling drug release<sup>12-15</sup>. To date, MSN delivery applications primarily use intravenous injection (IV). While IV is a well-established therapy for nanocarrier drug delivery, inhalation represents a highly desirable route of delivery to specifically target the respiratory system. Respiratory diseases also currently rank among the top ten causes of death globally<sup>16</sup>. Current research in MSN therapeutics has demonstrated that inhalation is a possible route of delivery, specifically for lung cancer<sup>17</sup>, as well as for novel applications for the treatment of tuberculosis<sup>13</sup>. Efficient and sustained delivery of therapeutic compounds carried and retained in the lungs for controlled release also represents a new approach for treatment.

The purpose of this study was to generate a functional aerosol containing unaggregated forms of MSN with the potential to be equipped with a broad-range of disease-targeting components<sup>15</sup>. The specific goals of the study were creation of suitable aerosolization conditions, verification of limited-to-no toxicity, while demonstrating MSN integrity to widely deliver nano bio-functional components to highly diverse regions of the respiratory tract. To optimize drug delivery and deposition in all areas of the respiratory tract, MSN was suspended in nanopure water and aerosolized in droplets in the respirable size range (0.1 to 3.0  $\mu\text{m}$ ). A mouse-model was used to test the inhalability of MSN. The effectiveness of the design was evaluated on the basis of deposition in pulmonary tissues, as well as cells collected from the entire respiratory tract and imaged with fluorescent and electron microscopy. Toxicity at each level of the respiratory tract was evaluated to assess acute toxicity of the combined nano-aerosol delivery biotechnology. To our knowledge, this represents the first comprehensive safety profile of aerosolized MSN in an *in vivo* inhalation model.

## Methods

### MSN Synthesis

The synthesis of 50 nm mesoporous silica nanoparticles was based on a previously published method<sup>15</sup>. Briefly, 250 mg cetyltrimethylammonium bromide (CTAB) and 220 mg Pluronic F127 was mixed with 120 mL of H<sub>2</sub>O, to which 875  $\mu$ L of 2M NaOH aqueous solution was added. The solution was kept at 80 °C before 1.2 mL of tetraethyl orthosilicate (TEOS). This was followed by an addition of 300  $\mu$ L of trihydroxysilylpropyl methylphosphonate after 30 min. The resulting suspension was then stirred for 2 hr and the particles were collected by centrifugation. The particles were then resuspended in a solution of 60 mL methanol with 60 mL of H<sub>2</sub>O and mixed with 0.8 g of NH<sub>4</sub>NO<sub>3</sub>. After stirring for 30 min at 60°C, the particles were centrifuged and washed with methanol.

### Polymer Coating and Fluorescent Labeling

To perform polymer coating, 100 mg of particles were suspended in 10 mL of 2.5 mg/mL polyethyleneimine (PEI) ethanolic solution and the solution was stirred at room temperature for 30 min. The particles were collected by centrifugation and washed with ethanol. 20 mL of anhydrous dimethylformamide (DMF) was used to resuspend the PEI-treated particles, and 1 mg of fluorescein isothiocyanate (FITC) N-hydroxysuccinimide (NHS) ester was added into the solution. 12 hr later, 500 mg of activated m-polyethylene glycol (PEG) was added and the solution was stirred for another 12 hr. The resultant particles were centrifuged and washed with DMF, methanol and water. The final suspension of MSN for aerosolization and inhalation studies was in nanopure water.

### Physiochemical Characterization

Images were taken using a JOEL 1200 transmission electron microscope. Nanoparticles were suspended into a 50  $\mu$ g/mL methanol suspension. Approximately 20  $\mu$ L of the solution was then used for sample preparation. Dynamic light scattering was performed on a ZetaSizer Nano (Malvern Instruments Ltd., Worcestershire, UK) using a 40  $\mu$ g/mL aqueous suspension to determine the particle size.

### MSN Aerosol Generation

A nanopure water droplet aerosol containing MSN nano-particles was delivered simultaneously to individual mice during 5 hours using a version of a multi-port exposure apparatus<sup>18</sup>. This aerosol was generated using a MiniHeart nebulizer<sup>19</sup> (Westmed, Inc., Tuscon, AZ) operated at 39 psig with filtered compressed air. The nebulizer was placed in an ice-water bath at 0 °C to minimize evaporation. The output concentration of liquid aerosol was about 106  $\mu$ L per minute (with only 1 or 2  $\mu$ L per minute of water vapor with the nebulizer in an ice-water bath). The optimal concentration of the MSN nano-particles in the nebulizer to minimize foaming of the aerosol was found to be 4 mg/mL (4  $\mu$ g/ $\mu$ L), and the nebulizer output of MSN was 424  $\mu$ g/min in 2 L/min of air. Since there was no diluting air, the aerosol MSN concentration was 424  $\mu$ g/min divided by 2 L/min of air at 212  $\mu$ g/L. When entering the exposure chamber at ambient temperature of about 25 °C, the water droplet aerosol had a mass median aerodynamic diameter of about 1.8  $\mu$ m.

The mass of aerosolized particles deposited in the lungs of a mouse was estimated by multiplying the amount inhaled by the deposition fraction for the selected region of the respiratory tract<sup>20</sup>.

The droplet deposition in the mouse respiratory tract in this study can be calculated by: Dose deposited =  $fctv$ , where:

$f$  = fraction deposited in respiratory tract region (function of particle size) given for the mouse pulmonary region as 0.08 for 1.8  $\mu\text{m}$  diameter water droplets<sup>20</sup>.

$c$  = aerosol MSN concentration (micrograms per liter of air): 212  $\mu\text{g/L}$ .

$t$  = time of aerosol treatment (minutes): 300 minutes.

$v$  = inhaled minute volume of air for mice (0.03 L for a 35 g mouse)

The calculated total MSN deposition in mice was approximately 140  $\mu\text{g}$  in the gas exchange pulmonary region of the lung, approximately 120  $\mu\text{g}$  in the tracheal and bronchial regions, and approximately 720  $\mu\text{g}$  in the head. About 40% of the inhaled aerosol was exhaled<sup>20</sup>.

### Aerosol Sampling

MSN size distribution during mouse inhalation exposure was measured using a cascade impactor (CI) connected to the nose-only exposure chamber. The CI was used as an aerosol sampling device containing 8 stages that measured aerosol sizes (mass median aerodynamic diameter) ranging from 0 – 4.66  $\mu\text{m}$ . Three sets of CI samples were collected during the mice inhalation exposure process. Each CI filter sample was taken at 1 L/min flow-rate for a 30 minute duration. The mass of MSN collected on the filters from the CI was used to determine MSN water droplet aerosol size distributions. Each filter (25 mm Pallflex) (VWR, Westchester, PA) was pre and post-weighed to determine the mass of aerosolized materials collected on the filter. Filters were analyzed using scanning electron microscopy (SEM) (FEI/Philips XL30 SFEG) to determine surface morphology. Composition was analyzed with an EDAX x-ray detector for energy-dispersive x-ray spectroscopy (EDS). Point-to-plane electrostatic precipitator samples were collected to study aerosol morphology using transmission electron microscopy (TEM).

### Animals

Thirty-two 8-week old male CD-1 mice (33–40 g) (Harlan, Livermore, CA) free of respiratory disease were used throughout this study. The mice were assigned by random selection into 4 groups of equal size, consisting of two treatment groups (filtered and MSN-exposed) and two time-points (1 and 7 days post-exposure) ( $n = 8/\text{group}$ ). Animals were handled in accordance with the U.S. Animal Welfare Acts as set forth in the National Institutes of Health guidelines, and the study was reviewed and approved by the UC Davis Institutional Animal Care and Use Committee. Mice were housed in plastic cages with TEK-Chip pelleted bedding. Water and feed (LabDiet 5001 rodent diet, Labdiet, Brentwood, MO) were accessible *ad libitum* except during the exposure period.

### **MSN Treatment in Mice**

Mice (n=8) per time-point (1 and 7 days) were exposed in the nose-only exposure system for 5 hours continuously. The exposed animals were treated with aerosolized MSN in nanopure water droplets. The control animals (n=8) per time-point, were also housed in nose-only exposure housing and received filtered air only. Animals were examined 1 day or 7 days post-exposure. The necropsy times were selected to measure acute responses to approximate the immediate and 1 week post effects of receiving the aerosolized version of the MSN nano-carrier.

### **Collection of Bronchoalveolar Lavage**

One and 7 days after exposure to aerosolized MSN or filtered air, mice were euthanized by intraperitoneal injection of pentobarbital (120 mg/kg body weight). The trachea was cannulated, and the lungs were lavaged with  $\text{Ca}^{2+}/\text{Mg}^{2+}$ -free phosphate-buffered saline (PBS; pH 7.4). Three in-and-out (1 mL amounts) lavages were performed using the same aliquot to maximize recovery of cells. Bronchoalveolar lavage fluid (BALF) was centrifuged at 2000 rpm for 10 min at 4°C. The cell pellet was resuspended in 1.0 mL 0.9% saline and 100  $\mu\text{L}$  was used to determine total cell count and viability. Cell viability was measured by exclusion of trypan blue, an indicator of irreversible loss of plasma membrane integrity.

### **Preparation of Bronchoalveolar Lavage Fluid (BALF) for Confocal Imaging**

The BALF was centrifuged using a Shandon Cytospin (Thermo Shandon, Inc., Pittsburgh, PA) to form a cell pellet, then subsequently resuspended in PBS to prepare cytospin slides. BALF cytospin slides were stained with DAPI (Molecular Probes, Eugene OR), a blue nuclear counterstain used for multicolor fluorescent techniques and coverslipped with AquaPoly/Mount (Polysciences, Inc., Warrington, PA), a water-soluble non-fluorescing mounting medium that retains and enhances fluorescent stains. BALF cytospin slides were analyzed for MSN uptake with confocal microscopy (Zeiss LSM 710, Jena, Germany, Plan ApoChromat 20 $\times$ /0.8 NA objective).

### **Preparation of BALF for Cell Differential Analysis**

BALF cytospin slides were stained with Dippkwik (American Mastertech Scientific, Lodi, CA) and were quantitatively analyzed for cell type. Macrophages, neutrophils, eosinophils, and lymphocytes were counted using light microscopy (500 cells per sample).

### **Preparation of BALF for TEM Imaging**

BALF cell pellet was resuspended in 2% agarose was fixed in 1/4 strength Karnovsky's fixative for TEM imaging. Alveolar macrophages were prefixed with 2.5% glutaraldehyde and postfixated in 1% osmium tetroxide. Specimens were embedded in Epon 812 after dehydration, and the ultrathin sections were stained with uranyl acetate and lead citrate for examination by transmission electron microscopy (TEM).

### **Lung Tissues Sections**

The left lung was inflation-fixed with 4% paraformaldehyde at 30 cm of water pressure for 1 hr. The lung was sliced into pieces and placed into cassettes. The lung pieces were then

dehydrated in a series of graded ethanol and embedded in paraffin. Paraffin-embedded lung tissue was cut into 5  $\mu\text{m}$  thick sections.

### **Confocal Imaging in Lung Tissue**

Lung tissue sections were mounted on slides using aquapolymount and a #1.5 coverslip. The presence of MSN particles in tissues was detected by confocal microscopy (Zeiss LSM 710, Jena, Germany, Plan Apochromat 20 $\times$ /0.8 NA objective) using appropriate excitation (488nm laser) and a spectral emission range (500–600nm). To differentiate between the 520nm peak of the FITC probe and the tissue autofluorescence, linear unmixing was performed by collecting spectral data from 500nm to 600nm in 9nm steps. The characteristic curve of the FITC fluorophore can easily be separated from the broader emission curve of the autofluorescence using linear unmixing<sup>21</sup>, which applies a linear algebra routine to every pixel in the image and assigns the percentage of each component to a separate channel. Thus, the autofluorescence can be “subtracted” out of the FITC signal.

### **Histopathology in Lung Tissue**

Lung tissue sections were stained with hematoxylin and eosin (H&E) and coverslipped with Clearmount. Airways and lung parenchyma were examined for the presence of cellular changes and inflammation with light microscopy. Lung tissue sections were stained with alcian blue and period acid Schiff (AB-PAS) (American Mastertech, Lodi, CA), and analyzed for the presence of mucin proliferation with light microscopy as a possible indication of airway epithelial cell irritation and mucosubstance production.

### **Nose Tissue Sections for Histopathology**

The nasal cavity was fixed in 4% paraformaldehyde, decalcified, and embedded in paraffin. Nasal tissue sections were stained with ABPAS and analyzed for mucin production.

### **Cell Differentials to Assess Possible Toxicity**

Three hundred cells from prepared cytospin slides for each animal were counted and categorized as macrophage, neutrophil, lymphocyte or eosinophil using light microscopy and a cell counter.

### **Statistical Analysis**

All numerical data were calculated as the mean and standard deviation. Analysis of variance was performed between treatment and control groups. Comparisons were considered significant if a value of  $p < 0.05$ . Statistical analysis was performed with JMP (SAS Institute, Inc., Cary, NC).

## **Results**

### **MSN platform design and characterization**

To make feasible delivery of a broad-based MSN complex over a wide range of target sites within the respiratory tract without compromising safety features or changing other structures in a nano-platform, a unique formulation of MSN was chosen that consisted of the

following: 50 nm silica cores with 2 nm mesopores and PEI-PEG copolymer coatings to ensure their aqueous stability and dispersibility. The hydrodynamic size of these nanoparticles was approximately 70 nm, which is believed optimal for a variety of biomedical applications. The nanoparticles were functionalized with a fluorescence tag, fluorescein isothiocyanate (FITC) N-hydroxysuccinimide (NHS), for ready detection following deposition in the respiratory tract.

### MSN aerosol generation

Because the fraction of inhaled aerosol deposited in each region of the mouse respiratory tract is a function of nanopure water aerosol droplet size distribution, a 1.8  $\mu\text{m}$  mass median aerodynamic diameter aerosol size distribution was chosen to optimize lung deposition fractions to insure detectable amounts at various levels of the respiratory tract<sup>20</sup>. The total amount deposited in each region of the respiratory tract was calculated as a function of deposition fraction, concentration, exposure duration, and inhaled minute volume of air. Given an 8% pulmonary deposition fraction for a 1.8  $\mu\text{m}$  mass median aerodynamic diameter (MMAD) droplet aerosol, factors of concentration and exposure duration were optimized in order to create enough capacity for a delivery system. The total volumetric rate of aerosol provided an air-flow-rate suitable for mouse respiration. The inhalation process involved a 2 L/min flowrate with a 4 mg/mL input MSN suspension concentration for 5 hours for the mouse study. An input concentration administered to mice that inspire about 30L/min for a total duration of 5 hours at an 8% deposition fraction yielded about an average 140  $\mu\text{g}$  of MSN in the pulmonary region of each mouse.

Applying this strategy with an optimal concentration of 4 mg/mL of MSN in suspension to minimize foaming due to PEI-PEG copolymer coating of MSN, resulted in MSN aerosol droplets with a wide size distribution (Figure 1). These droplets were in respirable range, and inhaled MSN congregates were found present in the gas-exchange region at both 1 and 7 days postexposure.

### In-vivo evidence that intact MSN aerosol reaches respiratory regions important for disease targeting

To determine whether aerosolized MSN reached and were retained in the respiratory tract, necropsies of mice 1 and 7 days were performed after receiving nose-only delivery of aerosolized MSN via the procedure as described above. Bronchoalveolar lavage fluid (BALF) cells were composed of more than 98% alveolar macrophages, many of which contained MSN at both 1 and 7 days post-inhalation (Figure 2) within alveolar macrophages. Using TEM imaging of BAL cytospin pellets, alveolar macrophages were confirmed to contain MSN fluorescentpositive inclusions at 1 day and 7 days (Figure 3). Intact MSN were found compartmentalized in phago-lysosomes at 1 day (Figure 3a, b) and 7 days (Figure 3c, d).

These results suggest that nanopure aerosol water droplet delivery of MSN effectively reaches the bronchial tree and gas exchange regions of the respiratory tract. Such regions are important targets for disease applications that require airway and alveolar lung penetration to achieve target site delivery, as well as systemic delivery via a very large surface area for

uptake and translocation to the underlying capillary bed. Such applications can be advantageous by bypassing gastrointestinal tract adsorption and/or liver metabolism.

Alveolar macrophage uptake of MSNs may also represent a critical step to target respiratory inflammatory diseases via macrophage-directed nanoparticle delivery system pathways. Phagolysosomes, an essential organelle of the macrophage, are ideal sub-cellular targets for MSN facilitated drug delivery. Chemical stimuli, such as pH, activate the mechanized controlled release systems utilized in MSN delivery systems. It has been shown that acidic phagolysosomes can protonate and activate accessible MSN surface groups. This “proton sponge effect” allows particles to escape endosomes and enables membrane impermeable payloads, such as nucleic acids and hydrophilic drugs, to be released from the membrane-bound compartments and travel to their effective sites<sup>1</sup>. Thus, aerosol droplet MSN delivery into phago-lysosomes without damage to MSN structures is consistent with this bypass of the endosome and suggests that MSN controlled-release drug delivery mechanisms can be directly applied to diseases affecting the respiratory system via inhalation.

### **In-vivo evidence that acute inhalation of MSN aerosol droplets is safe**

Possible toxicity of MSN was evaluated using tissue sections and collected cell samples from control and exposed mice 1 and 7 days post-exposure. No changes in the anatomy or epithelial cell composition were noted for the nasal cavity, bronchial airways or alveolar lung parenchyma following in mice exposed to MSN compared to control mice exposed to filtered air.

Histopathological analysis of lung tissues demonstrated normal centriacinar regions devoid of inflammatory cells in either sham control or MSN-exposed groups 1 and 7 days post exposure (Figure 4), although it should be noted these images were taken after lung lavage had been performed.

*In-vivo* cytotoxicity assessment was also performed. A quantitative assay was used to assess airway inflammation. Differential cell counts (macrophages, neutrophils, lymphocytes and eosinophils) were evaluated in BALF cells. BAL cells were found to be almost exclusively alveolar macrophages in mice exposed to MSN. The number of BAL cells recovered from the lungs was not significantly different in control mice or mice exposed to MSN, suggesting little-to-no evidence of MSN-induced inflammation or toxicity following a single 5-hour exposure 1 or 7 days following post-exposure (Figure 5). Macrophages were the predominant (>98%) cell type recovered by BAL. The lack of neutrophils, eosinophils, and lymphocytes in BAL are consistent with the absence of an acute inflammatory response to MSN exposure. Of interest, by 7 days post-exposure, all mice (n=8) which had been exposed to MSN continued to demonstrate a high frequency of fluorescently-tagged MSN inclusions in alveolar macrophages recovered by BAL (Figure 6).

## **Discussion**

We demonstrate in this study that PEI-PEG coated 50 nm MSN and suspended in nanopure water can be effectively aerosolized in a standard medical nebulizer. Aerosolization does not disrupt the mesoporous structure, which suggests that this method is an appropriate way to



administer MSN without damaging its unique nanoscale features. Moreover, MSN compatibility in a standard medical nebulizer indicates that this particular form of MSN administration may be easily applied to clinical settings. Surface coating is an important physiochemical parameter that determines the fate, biological effects, and toxicology of nanoparticles. PEI-PEG coated MSN behaved as single particles in nanopure water prior to nebulization due to the coating's electrostatic repulsion and suggests that MSN remained suspended as single particles in the nanopure water droplets during aerosol generation. However, water evaporated for imaging purposes results in MSN agglomeration and thus, the TEM image of aerosolized MSN only provides information on the number of MSN particles suspended in each droplet.

The purpose of this study was to generate a functional aerosol form of MSN with the potential to be equipped with a broad-range of disease targeting components. Using MSN with appropriate aerosol generating conditions, we accomplished non-toxic delivery of these unaggregated structures to all regions of the respiratory tract. In addition, the MSN were stable and present one-week post inhalation. These findings create an excellent collective framework to expand MSN platforms to a wide range of respiratory therapeutics and a more efficient and reliable delivery for existing therapies with current state-of-the art MSN-based inhalation nanobiotechnology.

To ensure the optimal MSN inhalation delivery, a complete inhalation procedure was designed that includes calculations of MSN input liquid concentration, nebulized MSN output aerosol droplet concentration, aerosol droplet size distribution, mouse inspiration rate, mouse lung volume, aerosol flow-rate, respiratory tract deposition efficiency, temperature manipulations, sample timing and exposure duration. Moreover, the mass of aerosolized particles deposited in the mouse lung was estimated by multiplying the total amount inhaled by the deposition fraction for the selected region of the respiratory tract<sup>20</sup>. The five hour exposure duration provided sufficient time to collect aerosol mass and size distribution data to evaluate the delivery effectiveness, stability, and structural integrity of the nano-aerosol technology for applications in a biological system. This protocol provides a long-lasting delivery capability to further expand the in-vivo MSN delivery strategies for therapeutic pulmonary disease treatment.

MSN have been demonstrated to be stable in aqueous solution and suitable for IV injection<sup>15</sup>. However, traditional aerosolization processes have not produced appropriate MSN aerosols because the PEI-PEG copolymer coating disrupts the aerosolization process by foaming the input solution and rendering it unable to further generate aerosols. We overcame this problem by optimizing the concentration of coated MSN in suspension using the methods described in the Experimental Section (*Polymer Coating and Fluorescent Labeling* and *MSN Aerosol Generation*). Since the fraction of inhaled aerosol droplet deposited in each region of the mouse respiratory tract is a function of aerosol particle size distribution<sup>20</sup>, the utilized set of MSN aerosol droplets caused them to reach different depths and sites of the pulmonary tract. Hence, the potential exists for delivery targeting for a wide range of pulmonary diseases.

Mice are compulsive nose breathers having very shallow inhalation volumes per breath and numerous breaths per minute since oxygen diffusion is a major factor in their lung ventilation. Deposition of aerosol droplets in the deep lung in mice is less than 10% for 1 micrometer water droplets and close to zero for droplets larger than 3 micrometer<sup>20</sup>.

In sharp contrast, people can be treated trans-orally with a tidal volume of 750 mL at 15 breaths per minute with larger droplets up to 10 micrometer containing much larger numbers of nanoparticles and depositing up to 50% of droplets in the pulmonary alveolar region of the lungs. Therefore, the 300-minute aerosol nasal treatment with mice in this study can be equated to a 3-minute trans-oral treatment in humans.

Our analyses indicate that delivery of MSN carriers to the respiratory system via inhalation does not result in acute toxicity. The cellular internalization of MSN after inhalation suggests that the aerosol droplet form of MSN carriers can be directed to both the lung tissue and lung macrophages. Macrophages have been used as suitable vehicles to carry nanoparticles and drugs to target inflammatory diseases<sup>13, 22–25</sup>. Aerosolized MSN compatibility with pulmonary macrophages expands the utility of such a system for treatment of diseases caused by intracellular pathogens in the lung. The MSN in this study concentrated in macrophage phagolysosome compartments, which was expected. Some studies demonstrated that MSNs derivatized with pH-responsive nanovalves release their cargo molecules in acidic lysosomal environments<sup>3</sup>. Targeting alveolar macrophages is a critical cell type that takes up MSN following short-term inhalation.

Both qualitative and quantitative toxicity analyses provided evidence that short-term MSN inhalation treatment did not cause acute pulmonary inflammation. Other studies show that sol-gel synthesized MSN is safe, and the addition of polymer coatings further screens surface silanols from interacting with cell membranes, preventing membranolysis<sup>26</sup>. The lack of acute toxicity in this coated MSN aerosol model is agreement with *in vivo* studies that demonstrate polymer coated MSN delivered through other routes of exposure produce no toxicity. This suggests that the MSN aerosol based delivery technology may be a promising form of inhalation nanobiotechnology compatible with the entire respiratory tract for therapeutic purposes. Delivering nano-carriers to the alveolar airspaces can provide a route to target the deep lung and numerous alveolar macrophages. An inhalable nano-carrier that can reach alveolar macrophages can facilitate drug delivery for a wide variety of inflammatory and infectious diseases of the lung. Delivering nano-carriers to the nasal cavity may also provide direct nose to brain transport via the olfactory nerve, which could facilitate drug delivery for diseases affecting the central nervous system. Therefore, the developed inhalation-based delivery system that delivers an aerosol carrier with a multifunctional MSN platform to the entire respiratory tract is beneficial.

Our results indicate that aerosol droplet delivery of MSN effectively reaches the bronchial tree and gas exchange regions of the respiratory tract. These regions are important targets for disease applications that require airway and alveolar lung penetration to achieve target site delivery, as well as systemic delivery via a very large surface area for uptake and translocation to the underlying capillary bed. These applications have the advantage of bypassing gastrointestinal tract adsorption and/or liver metabolism.

In conclusion, a novel nanocarrier aerosol droplet delivery strategy was developed and implemented. We used a MSN inhalation platform without modification of nanocarrier architecture. Our work provides the first demonstration of an aerosol delivery method that maintains the structural integrity of MSNs following aerosolization. The capacity to broadly apply drug-carrier inhalation nanotechnology to the various regions of the respiratory tract from the nasal passages to the airways and alveoli may potentially be of great benefit to treating a broad range of diseases including allergies, lower respiratory infections, and chronic obstructive pulmonary disease<sup>27, 28</sup>. Our work provides the basis for further human study of the appropriate MSN aerosol dosage, stability, structural integrity, pressure, and timing for respiratory therapy.

## Acknowledgements

### *Supporting Information*

This work was supported in part by NIH-NIEHS Grant R25 Short-Term Educational Experiences for Research (STEER), NIEHS grant U01 ES 020127 and NIOSH grant 0H07550 to study the fate and transport of inhaled nanoparticles in the respiratory tract. We also wish to acknowledge the Gordon and Betty Moore Foundation and the Blacutt-Underwood Endowed Chair for support in imaging resources and Mr. Siyang Li for graphics.

## References

1. Li ZX, Barnes JC, Bosoy A, Stoddart JF, Zink JJ. Mesoporous silica nanoparticles in biomedical applications. *Chemical Society Reviews*. 2012; 41(7):2590–2605. [PubMed: 22216418]
2. Mamaeva V, Sahlgren C, Linden M. Mesoporous silica nanoparticles in medicine—Recent advances. *Advanced Drug Delivery Reviews*. 2013 May; 65(5):689–702. [PubMed: 22921598]
3. Angelos S, Liang M, Choi E, Zink JJ. Mesoporous silicate materials as substrates for molecular machines and drug delivery. *Chemical Engineering Journal*. 2008 Mar; 137(1):4–13.
4. Douroumis D, Onyesom I, Maniruzzaman M, Mitchell J. Mesoporous silica nanoparticles in nanotechnology. *Critical Reviews in Biotechnology*. 2013 Sep; 33(3):229–245. [PubMed: 22724458]
5. Idris NM, Gnanasammandhan MK, Zhang J, Ho PC, Mahendran R, Zhang Y. In vivo photodynamic therapy using upconversion nanoparticles as remote-controlled nanotransducers. *Nature Medicine*. 2012 Oct. 18(10):1580–U190.
6. Mai WX, Meng H. Mesoporous silica nanoparticles: A multifunctional nano therapeutic system. *Integrative Biology*. 2013; 5(1):19–28. [PubMed: 23042147]
7. Ferrari M. Cancer nanotechnology: Opportunities and challenges. *Nature Reviews Cancer*. 2005 Mar; 5(3):161–171.
8. Hom C, Lu J, Liang M, Luo HZ, Li ZX, Zink JJ, et al. Mesoporous Silica Nanoparticles Facilitate Delivery of siRNA to Shutdown Signaling Pathways in Mammalian Cells. *Small*. 2010 Jun; 6(11): 1185–1190. [PubMed: 20461725]
9. Popat A, Hartono SB, Stahr F, Liu J, Qiao SZ, Lu GQ. Mesoporous silica nanoparticles for bioadsorption, enzyme immobilisation, and delivery carriers. *Nanoscale*. 2011; 3(7):2801–2818. [PubMed: 21547299]
10. Popat A, Liu J, Hu QH, Kennedy M, Peters B, Lu GQ, et al. Adsorption and release of biocides with mesoporous silica nanoparticles. *Nanoscale*. 2012; 4(3):970–975. [PubMed: 22200056]
11. Lin CY, Chang YH, Li KC, Lu CH, Sung LY, Yeh CL, et al. The use of ASCs engineered to express BMP2 or TGF-beta 3 within scaffold constructs to promote calvarial bone repair. *Biomaterials*. 2013 Dec; 34(37):9401–9412. [PubMed: 24016854]
12. Guo HC, Feng XM, Sun SQ, Wei YQ, Sun DH, Liu XT, et al. Immunization of mice by Hollow Mesoporous Silica Nanoparticles as carriers of Porcine Circovirus Type 2 ORF2 Protein. *Virology Journal*. 2012 Jun.9

13. Clemens DL, Lee BY, Xue M, Thomas CR, Meng H, Ferris D, et al. Targeted Intracellular Delivery of Antituberculosis Drugs to Mycobacterium tuberculosis-Infected Macrophages via Functionalized Mesoporous Silica Nanoparticles. *Antimicrobial Agents and Chemotherapy*. 2012 May; 56(5):2535–2545. [PubMed: 22354311]
14. Wang MQ, Zhang JX, Yuan ZM, Yang WZ, Wu Q, Gu HC. Targeted Thrombolysis by Using of Magnetic Mesoporous Silica Nanoparticles. *Journal of Biomedical Nanotechnology*. 2012 Aug; 8(4):624–632. [PubMed: 22852472]
15. Meng H, Xue M, Xia T, Ji ZX, Tarn DY, Zink JI, et al. Use of Size and a Copolymer Design Feature To Improve the Biodistribution and the Enhanced Permeability and Retention Effect of Doxorubicin-Loaded Mesoporous Silica Nanoparticles in a Murine Xenograft Tumor Model. *Acc Nano*. 2011 May; 5(5):4131–4144. [PubMed: 21524062]
16. World Health Organization. The top 10 causes of death. WHO Media Centre. 2011. Contract No.: Fact Sheet 310. [http://www.who.int/mediacentre/factsheets/fs310\\_2008.pdf](http://www.who.int/mediacentre/factsheets/fs310_2008.pdf)
17. Taratula O, Garbuzenko OB, Chen AM, Minko T. Innovative strategy for treatment of lung cancer: targeted nanotechnology-based inhalation co-delivery of anticancer drugs and siRNA. *Journal of Drug Targeting*. 2011 Dec; 19(10):900–914. [PubMed: 21981718]
18. Raabe OG, Bennick JE, Light ME, Hobbs CH, Thomas RL, Tillery MI. Improved apparatus for acute inhalation exposure of rodents to radioactive aerosols. *Toxicology and Applied Pharmacology*. 1973; 26(2):264–273. [PubMed: 4751105]
19. Raabe OG, Wong TM, Wong GB, Roxburgh JW, Piper SD, Lee JIC. Continuous nebulization therapy for asthma with aerosols of beta(2) agonists. *Annals of Allergy Asthma & Immunology*. 1998 Jun; 80(6):499–508.
20. Raabe OG, Al-Bayati MA, Teague SV, Rasolt A. Regional Deposition of Inhaled Monodisperse Coarse and Fine Aerosol Particles in Small Laboratory Animals. *Ann Occup Hyg*. 1988; 32:53–63.
21. Dickinson ME, Bearman G, Tille S, Lansford R, Fraser SE. Multi-spectral imaging and linear unmixing add a whole new dimension to laser scanning fluorescence microscopy. *Biotechniques*. 2001 Dec.31(6):1272-+. [PubMed: 11768655]
22. Zhang HY, Dunphy DR, Jiang XM, Meng H, Sun BB, Tarn D, et al. Processing Pathway Dependence of Amorphous Silica Nanoparticle Toxicity: Colloidal vs Pyrolytic. *Journal of the American Chemical Society*. 2012 Sep; 134(38):15790–15804. [PubMed: 22924492]
23. Jain, S.; Amiji, M. Macrophage-targeted nanoparticle delivery systems. In: Pru'dhomme, RK.; Svenson, S., editors. *Multifunctional nanoparticles for drug delivery applications: Imaging, targeting, and delivery*. New York: Springer Publishing; 2012. p. 47-84.
24. Attarwala H, Amiji M. Multi-Compartmental Nanoparticles-in-Emulsion Formulation for Macrophage-Specific Anti-Inflammatory Gene Delivery. *Pharmaceutical Research*. 2012 Jun; 29(6):1637–1649. [PubMed: 22281760]
25. McCarthy JR, Korngold E, Weissleder R, Jaffer FA. A Light-Activated Theranostic Nanoagent for Targeted Macrophage Ablation in Inflammatory Atherosclerosis. *Small*. 2010 Sep; 6(18):2041–2049. [PubMed: 20721949]
26. Tarn D, Ashley CE, Xue M, Carnes EC, Zink JI, Brinker CJ. Mesoporous Silica Nanoparticle Nanocarriers: Biofunctionality and Biocompatibility. *Accounts of Chemical Research*. 2013 Mar; 46(3):792–801. [PubMed: 23387478]
27. Thorley AJ, Tetley TD. New perspectives in nanomedicine. *Pharmacology & Therapeutics*. 2013 Nov; 140(2):176–185. [PubMed: 23811125]
28. Slowing II, Wu CW, Vivero-Escoto JL, Lin VSY. Mesoporous Silica Nanoparticles for Reducing Hemolytic Activity Towards Mammalian Red Blood Cells. *Small*. 2009 Jan; 5(1):57–62. [PubMed: 19051185]

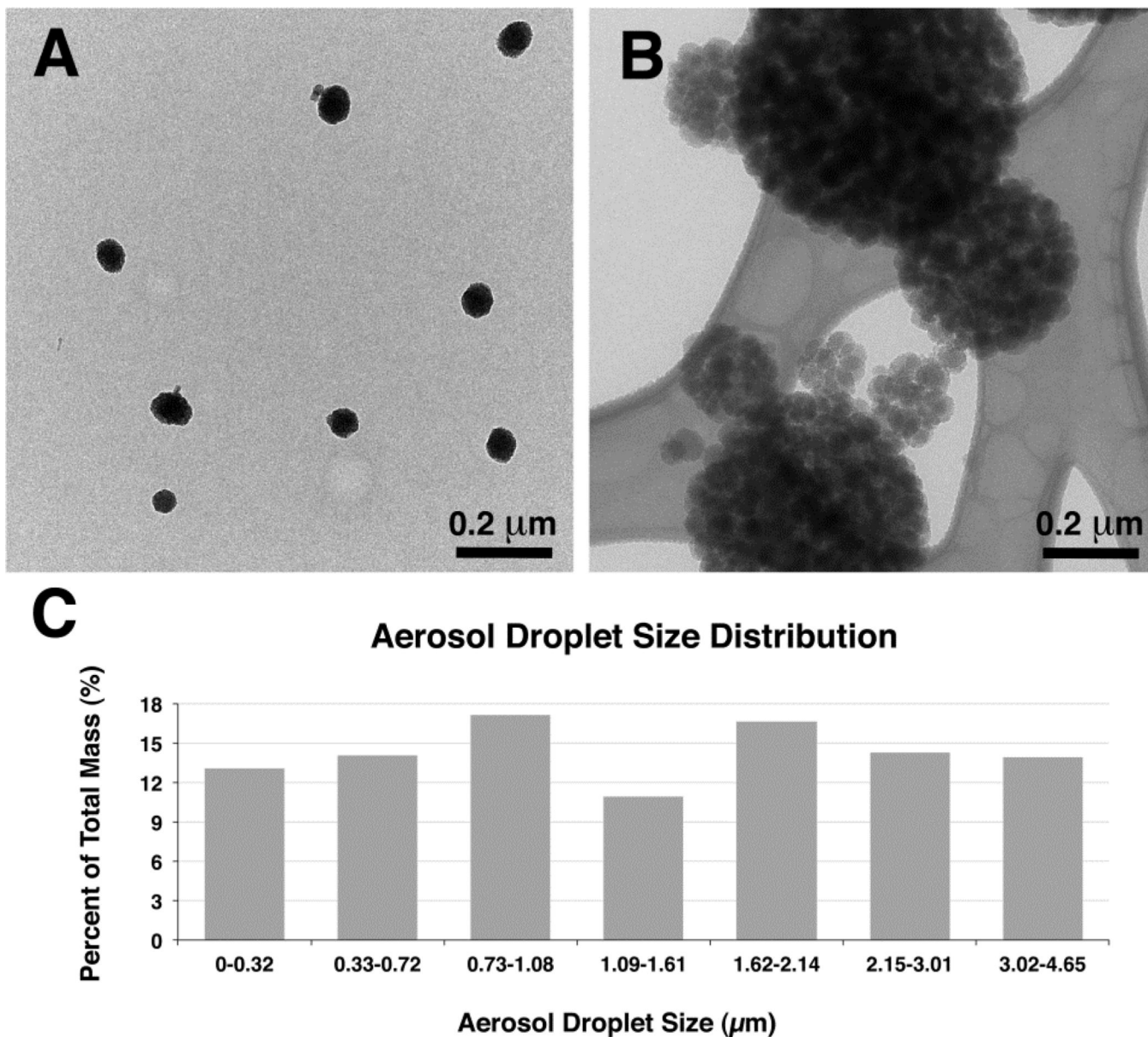


**Figure 1.** Functionalized mesoporous silica nanoparticles (MSN) aerosol generation for inhalation. (a) Pre-aerosolized MSN by transmission electron microscopy (TEM) demonstrating single MSN that had been suspended in aqueous solution (scale bar: 0.2  $\mu\text{m}$ ). (b) TEM image of dried aerosol droplets of different sizes containing different quantities of nanoparticles due to water droplets of variable size following nebulization (scale bar: 0.2  $\mu\text{m}$ ). (c) A wide range of MSN aerosol droplet size distribution was observed to enhance particle deposition throughout the entire respiratory tract as measured by gravimetrics.

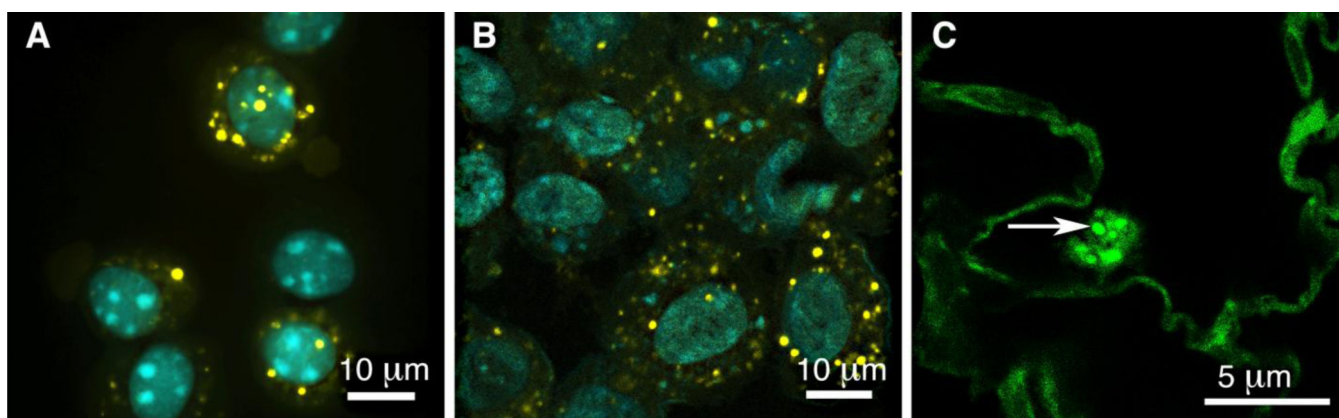


**Figure 2.** Confocal imaging of fluorescently labeled MSN (yellow) in alveolar macrophages recovered from bronchoalveolar lavage fluid (BALF) at 1 (a) and 7 (b) days post-inhalation (scale bar: 10  $\mu\text{m}$ ). Cell nuclei are stained blue. (c) MSN present in an alveolar macrophage found in an alveolar airspace in the gas exchange region of the lungs (scale bar: 0.5  $\mu\text{m}$ ). Arrow points to fluorescent MSN inclusion in an alveolar macrophage. Mice: n=8 / time-point.

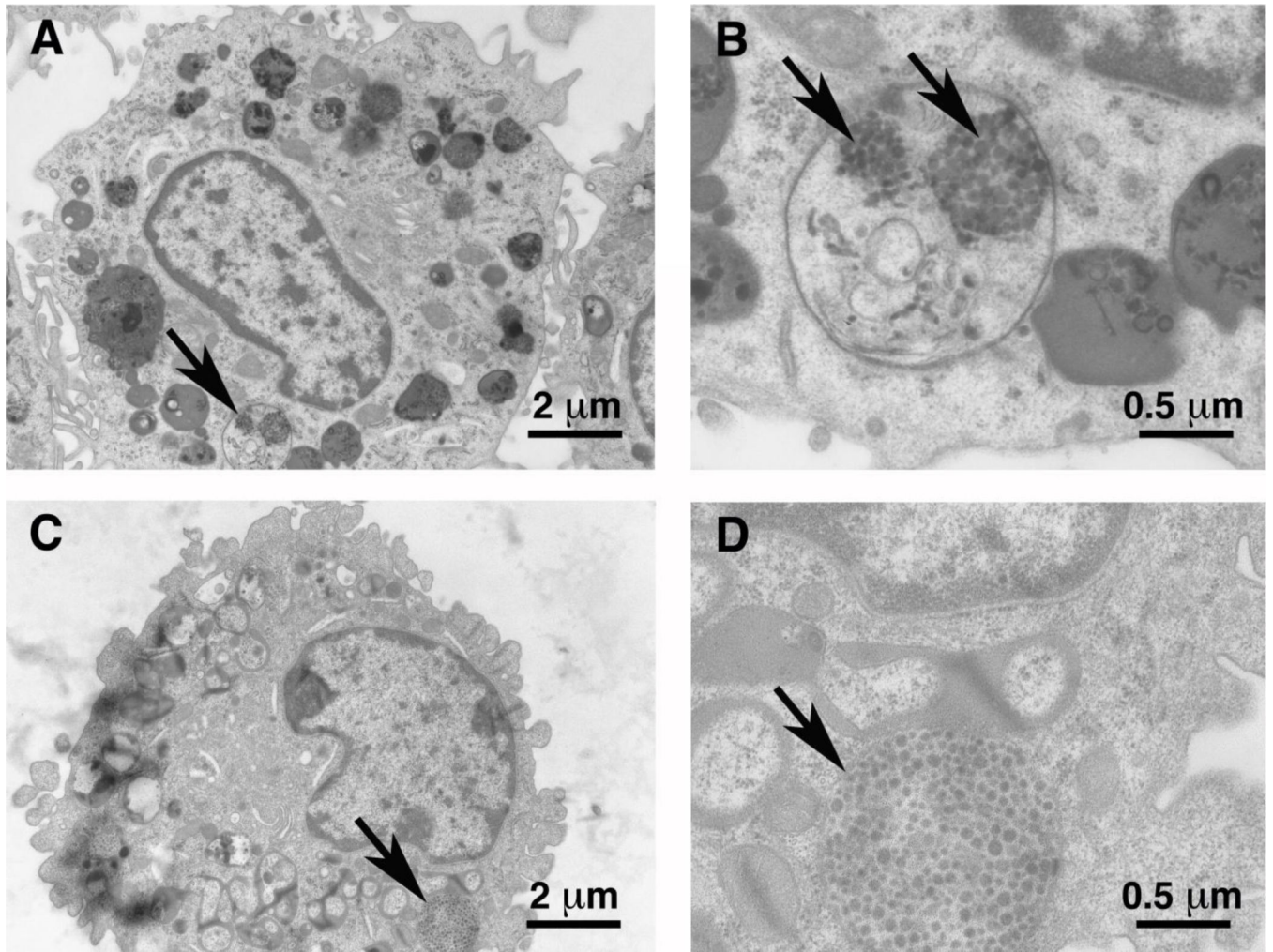


**Figure 3.** Transmission electron micrographs of MSN internalization in alveolar macrophages recovered from lungs at 1 day (a,b) and 7 days (c,d) post-inhalation. The arrows point to the position of the MSN complexes within phagolysosomes of the cell (scale bar: 2 μm: a,c) (scale bar: 0.5 μm, b,d). Mice: n=8 / time-point.

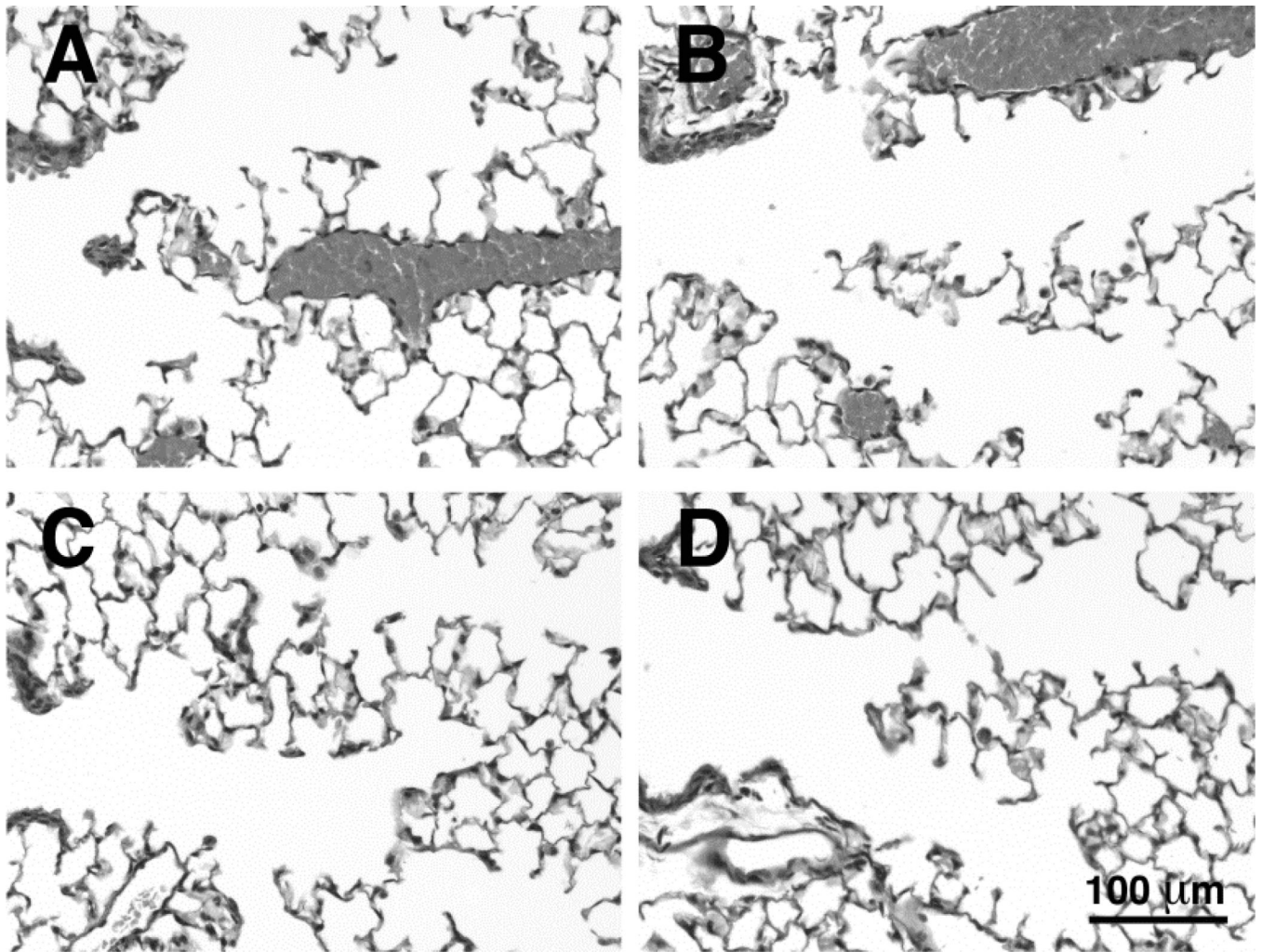


**Figure 4.** Bright-field microscope images of the bronchiole-alveolar duct (centriacinar) regions of the lung at 1 day (a, b) and 7 days (c, d) post-inhalation for sham control animals (a, c) and MSN-exposed mice (b, d). All groups demonstrate normal histology of the lungs and the absence of inflammatory cells within the bronchial, centriacinar or more distal alveolar regions of the lungs. However, it should be noted these images were taken after BAL had been performed. Scale bar: 100  $\mu\text{m}$ . Control mice: n=8 / time-point; MSN mice: n=8 / time-point.



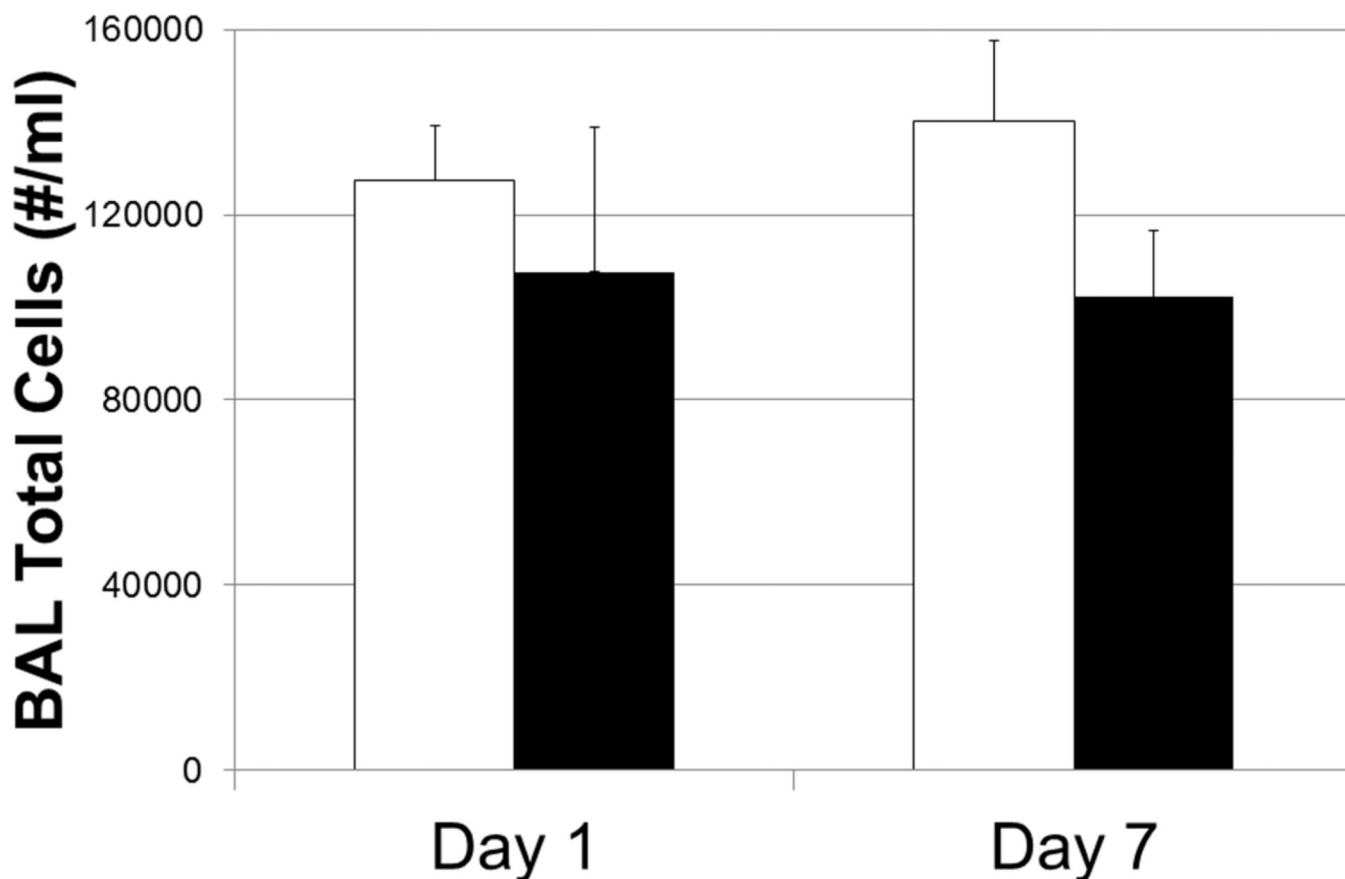


**Figure 5.**

Total cell number recovered by BAL from the lungs (#/ml). Greater than 98% of the cells recovered by BAL were alveolar macrophages. There was no significant difference in total cell numbers between control (open bars) and MSN-exposed mice (closed bars). Numerous macrophages were found to contain fluorescent-labelled MSN at both 1 and 7 days following inhalation. No obvious injury was observed with all BAL samples having greater than 95% cell viability in both control and MSN-exposed mice. Control mice: n=8 / time-point; MSN mice: n=8 / time-point.

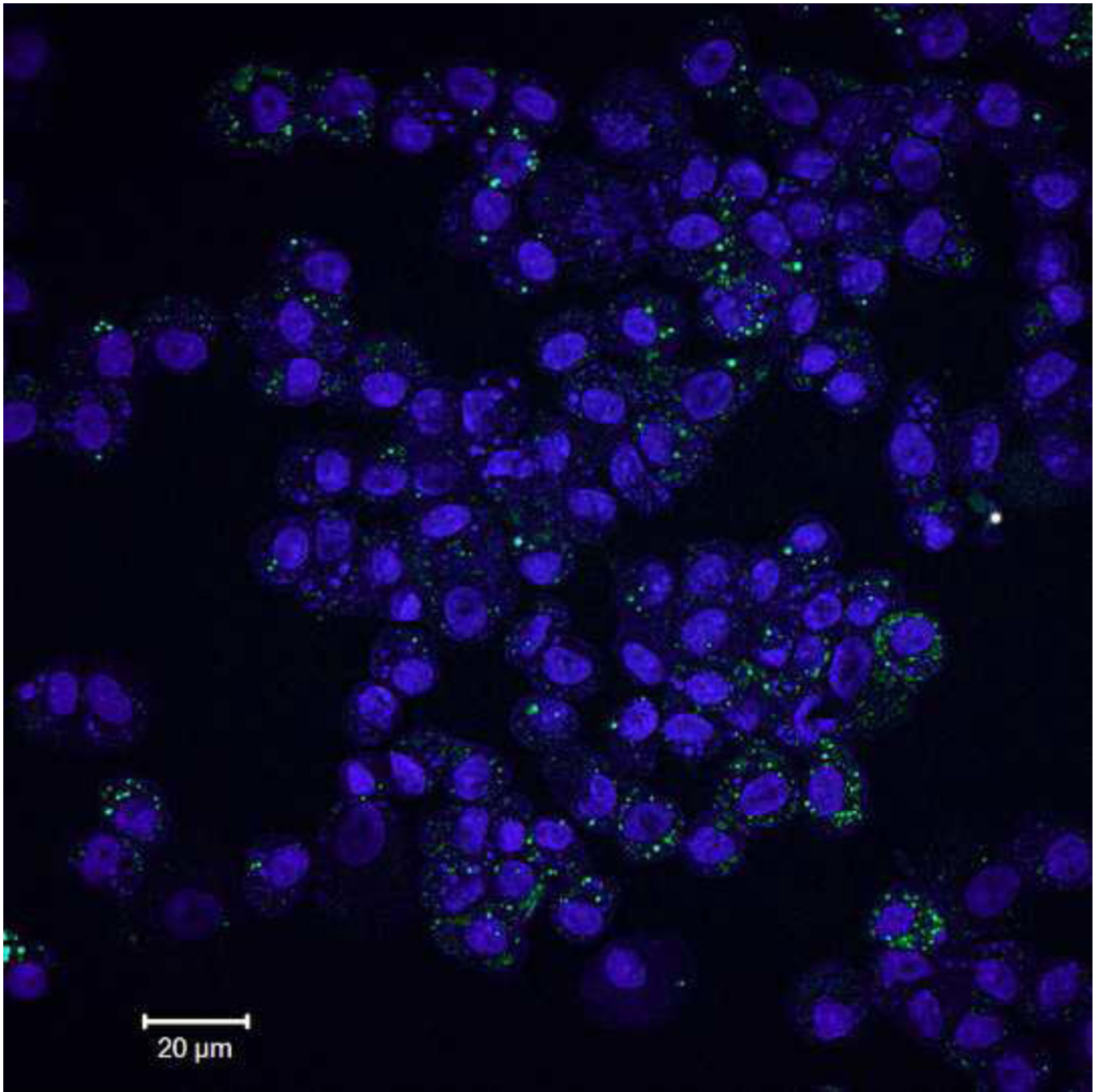


**Figure 6.** Low magnification light micrograph of cells recovered by bronchoalveolar lavage 7 days post-inhalation. Virtually all cells contain to some degree fluorescently-tagged MSN (scale bar: 20  $\mu\text{m}$ ). MSN mice: n=8 / time-point.